

Optical Engineering

OpticalEngineering.SPIEDigitalLibrary.org

Application of the time-invariant linear filter approximation to parametrization of surface metrology with high-quality x-ray optics

Valeriy V. Yashchuk
Yury N. Tyurin
Anastasia Y. Tyurina

Application of the time-invariant linear filter approximation to parametrization of surface metrology with high-quality x-ray optics

Valeriy V. Yashchuk,^a Yury N. Tyurin,^{b,c} and Anastasia Y. Tyurina^d

^aLawrence Berkeley National Laboratory, Berkeley, California 94720, United States

^bMoscow State University, Moscow 119991, Russia

^cSecond Star Algonumerics, Needham, Massachusetts 02494, United States

^dScientific Systems, Woburn, Massachusetts 01801, United States

Abstract. We investigate the time-invariant linear filter (TILF) approach to optimally parameterize the surface metrology of high-quality x-ray optics considered as a result of a stationary uniform random process. The approach is a generalization of autoregressive moving average (ARMA) modeling of one-dimensional slope measurements with x-ray mirrors considered. We show that the suggested TILF approximation has all the advantages of one-sided autoregressive and ARMA modeling, allowing a high degree of confidence when fitting the metrology data with a limited number of parameters. Compared to ARMA modeling, the TILF approximation gains in terms of better fitting accuracy and the absence of the causality limitation. Moreover, the TILF approach can be directly generalized to two-dimensional random fields. With the determined model parameters, the surface topography of prospective beamline optics can be reliably forecast before they are fabricated. These forecast metrology data, containing essential and reliable statistical information about the existing optics which are fabricated by the same vendor and technology, but generally, have different sizes, and slope and height root-mean-square variations, are vitally needed for numerical simulations of the performance of new x-ray beamlines and those under upgrade. © The Authors. Published by SPIE under a Creative Commons Attribution 3.0 Unported License. Distribution or reproduction of this work in whole or in part requires full attribution of the original publication, including its DOI. [DOI: [10.1117/1.OE.53.8.084102](https://doi.org/10.1117/1.OE.53.8.084102)]

Keywords: x-ray optics; surface metrology; statistical modeling; metrology parametrization; time-invariant linear filter; autoregressive moving average; surface topography forecasting.

Paper 140674P received Apr. 23, 2014; revised manuscript received Jul. 3, 2014; accepted for publication Jul. 16, 2014; published online Aug. 6, 2014.

1 Introduction

Development of new beamlines for third-generation synchrotron radiation sources and free electron lasers is reliant upon the availability of x-ray optics of unprecedented quality, with a surface slope accuracy in the range of 0.1 to 0.2 μrad and a surface height error of less than 1 nm.¹⁻⁵ The uniqueness of the optics and the limited number of proficient vendors makes the fabrication of such optics extremely time consuming and expensive. Therefore, it is essential to exactly provide the specifications for optic fabrication as is numerically evaluated for the required beamline performance, avoiding over- as well as under-specifications. Adequate numerical simulations of the performance of new beamlines and those under upgrade require refined and reliable information about the expected surface slope and height distributions of the planned x-ray optics before they are fabricated. Such information should be based on the metrology data from existing mirrors made by the same vendor, using the same technology, though the sizes, slope, and height root-mean-square (RMS) variations may be different.

In a classical work⁶ by Church and Berry, a comprehensive analysis of the problems and the limitations of reliable spectral estimations of the measured surface profile data were provided. The work also discussed a possibility for treating the random rough surface as the result of a stochastic

random process described by an autoregressive (AR) model. The surface description based on the AR model or the extended autoregressive moving average (ARMA) model^{7,8} provided a way to replace the spectral estimation problem with that of parameter estimation.

In recent works,^{9,10} ARMA modeling is applied to the surface slope metrology data obtained with the existing optics, allowing highly reliable forecasting of expected surface slope distributions of prospective x-ray optics, fabricated by the same vendor with the same technology.

A best-fit ARMA model has a limited number of parameters. The numerical values of the parameters and their confidence intervals can be determined with the use of standard statistical software. With the determined parameters of the ARMA model, the surface slope profile of an optic with a newly desired specification has been reliably forecast. The high accuracy of this type of forecasting has been demonstrated by comparing the power spectral density (PSD) distributions of the measured and forecast slope profiles.^{9,10}

In the present work, we investigate the time-invariant linear filter (TILF) approach to optimally parameterize the surface metrology of high-quality x-ray optics, which is thought of as a result of a stationary uniform random process. We show that the TILF approximation gains a better fitting accuracy and is free from the causality problem, compared to ARMA modeling of the surface metrology data. Therefore, the suggested TILF approach can be directly generalized to two-dimensional (2-D) random fields.

*Address all correspondence to: Valeriy V. Yashchuk, E-mail: vyashchuk@lbl.gov

This paper is organized as follows: In Sec. 2, we briefly review the mathematical fundamentals of one-dimensional (1-D) ARMA modeling of topography of random rough surfaces. In Sec. 3, we reproduce the results of ARMA fitting of the 1-D surface slope distribution of a high-quality reference mirror measured with a slope profiler. Here, we pay special attention to investigating the reverse symmetry of 1-D ARMA fitting of the slope data, and provide arguments for symmetrization of the modeling. Section 4 gives the mathematical fundamentals of modeling with TILFs. We also explain the relationships between 1-D ARMA and TILF models. Section 5 presents the results of the TILF modeling of a 1-D surface slope distribution of the reference mirror. We apply here a 1-D TILF transformation based on a symmetrization of the ARMA fit. Section 6 concludes the paper by summarizing the main concepts discussed throughout the paper and stating a plan for extending the suggested approach to parameterize the results of the 2-D surface metrology data.

2 One-Dimensional Autoregressive Moving Average Modeling of Random Rough Surfaces

We analyze the surface slope metrology with high-quality x-ray optics. For a 1-D case, the result of the metrology is a distribution (trace) of residual (after subtraction of the best fit figure and trends) slopes $\alpha[n]$ measured over discrete points $x_n = n \cdot \Delta x$ with uniform increment Δx ; $n = 1, \dots, N$, where N is the total number of observations, and $(N - 1)\Delta x$ is the total length of the trace.

ARMA modeling describes the distribution $\alpha[n]$ as a result of a uniform stochastic process:^{7,8}

$$\alpha[n] = \sum_{l=1}^p a_l \alpha[n-l] + \sum_{l=0}^q b_l \nu[n-l], \quad (1)$$

where $\nu[n]$ is the zero-mean unit-variance white Gaussian noise (white Gaussian noise) that is the driving noise of the model. The parameters p and q are the orders of the ARMA processes, respectively. At $q = 0$ and $b_0 = 1$, the ARMA process (1) reduces to an AR stochastic process. In addition to the linearity, an ARMA transformation is time invariant since its coefficients depend on the relative lags, l , rather than on n . The goal of the modeling is to determine the ARMA orders and to estimate the corresponding AR and MA coefficients a_l and b_l .¹¹⁻¹³ For ARMA analysis of the experimental data (Secs. 3 and 5), we use a standard statistical software, EViews 8.¹⁴ The software allows the determination of the ARMA model parameters, verifies the statistical reliability of the model, and simulates (forecasts) the new surface slope data corresponding to the determined ARMA model.

As Church and Berry discussed,⁶ ARMA fitting allows for the replacement of the spectral estimation problem by a problem of parameter estimation. In principle, the parameters of a successful ARMA model of a rough surface should relate to the polishing process. The analytical derivation of such a relation is a separate difficult task; there are only a few works that try to solve the problem.^{15,16} Instead, most of the existing work provides an empirical ARMA description of the results of the polishing processes.^{11,17} When an ARMA model is identified, the corresponding PSD distribution can be analytically derived:⁷

$$P_h(f) = \sigma^2 \frac{B[e^{i2\pi f}]B[e^{-i2\pi f}]}{A[e^{i2\pi f}]A[e^{-i2\pi f}]} = \sigma^2 \sum_{l=-\infty}^{\infty} r_h[l]e^{-i2\pi lf}, \quad (2)$$

where the frequency $f \in [-0.5, 0.5]$,

$$A[e^{i2\pi f}] = 1 + a_1 e^{i2\pi f} + \dots + a_p e^{i2\pi pf}, \quad (3)$$

$$B[e^{i2\pi f}] = b_0 + b_1 e^{i2\pi f} + \dots + b_q e^{i2\pi qf}, \quad (4)$$

and the autocorrelation function (ACF) of the surface profile is determined by Eq. (1). Eq. (2) can be expressed as

$$\begin{aligned} P_x(f) &= \sigma^2 \frac{(b_0 + b_1 z^{-1} + \dots + b_q z^{-q})(b_0 + b_1 z^1 + \dots + b_q z^q)}{(1 - a_1 z^{-1} - \dots - a_p z^{-p})(1 - a_1 z^1 - \dots - a_p z^p)} \\ &= \sigma^2 \sum_{l=-\infty}^{\infty} r_h[l]z^{-l}, \end{aligned} \quad (5)$$

where $z = e^{i2\pi f}$ and σ^2 is the variance of the driving noise $\nu[n]$. According to Eq. (5), $r_h[l]$ is a nonlinear function of the ARMA coefficients, a_l for $l = 1, \dots, p$, and b_l for $l = 1, \dots, q$.

A low-order ARMA fit, if successful, allows the parametrization of both the PSD and the ACF of a random rough surface. The PSD distributions appear as highly smoothed versions of the corresponding estimates via a direct digital Fourier transform (DFT).^{9,10} The description of a rough surface, as the result of an ARMA stochastic process, provides a model-based mechanism for extrapolating the spectra outside the measured bandwidth.^{9,10}

Trustworthy ARMA modeling and forecasting, based on a limited number of observations, assume the statistical stability of the data used. The data are statistically stable if they are the result of a so-called wide sense stationary (WSS) random process (see, Ref. 7). The process $\alpha[n]$, where $n = 1, \dots, N$, and N is the number of observations, is a WSS process if its ACF,

$$r_h[l] = E(\alpha[n]\alpha[n-l]), \quad (6)$$

only depends on the lag l , and does not depend on the value of n . In Eq. (1) E is the expectation operator. Note that the PSD of the WSS random process $\alpha[n]$ can be found from the ACF [compare with Eqs. (2) and (5)]:

$$P_h(f) = \sum_{l=-\infty}^{\infty} r_h[l]e^{-i2lf}. \quad (7)$$

Recent publications^{9,10} describe a successful application of the ARMA modeling to the experimental surface slope data for a 1280 m spherical reference mirror.^{18,19} The data were obtained with the Advanced Light Source developmental long trace profiler (DLTP).²⁰ The major reason for the data selection is their very high accuracy with a low contribution from random and systematic errors. The accuracy of the data has been verified in cross comparison with measurements performed with the HZB/BESSY-II nanometer (HZB/BESSY-II, Adlershof, Germany) optical component measuring machine (NOM),²¹⁻²³ one of the world's best slope measuring instruments. The difference of the NOM

and DLTP measurements does not exceed $\pm 0.15 \mu\text{rad}$; the RMS variation of the difference is 86 nrad .

3 Reverse Symmetry of One-Dimensional Autoregressive Moving Average Fitting of Surfaces Slope Measurements

Traces (a) and (b) in Fig. 1 reproduce the results of the ARMA modeling performed in Refs. 9 and 10. The measured residual slope trace, after subtracting the best-fit spherical surface shape with a radius of curvature of 1287.5 m , is shown with the short-dashed red line. The trace consists of $N = 547$ points measured with an increment of $\Delta x = 0.2 \text{ mm}$. The fitted slope trace, shown in Fig. 1(a) with the green long-dashed line, corresponds to the best-fitted ARMA model with the parameters given in Table 1.

The EViews' regression output in Table 1 contains the results of the application of several methods helpful for the evaluation of the reliability of the regression output. A value of $R^2 \approx 0.97$ indicates that the both regressions describe 97% of the data's variance. The Durbin-Watson statistic, a test for first-order serial correlation of the residuals, is ~ 2 , suggesting that there is no serial correlation. The low probabilities and the high t -statistics in the regression output indicate that AR(1), AR(4), MA(2), MA(6), and MA(3)

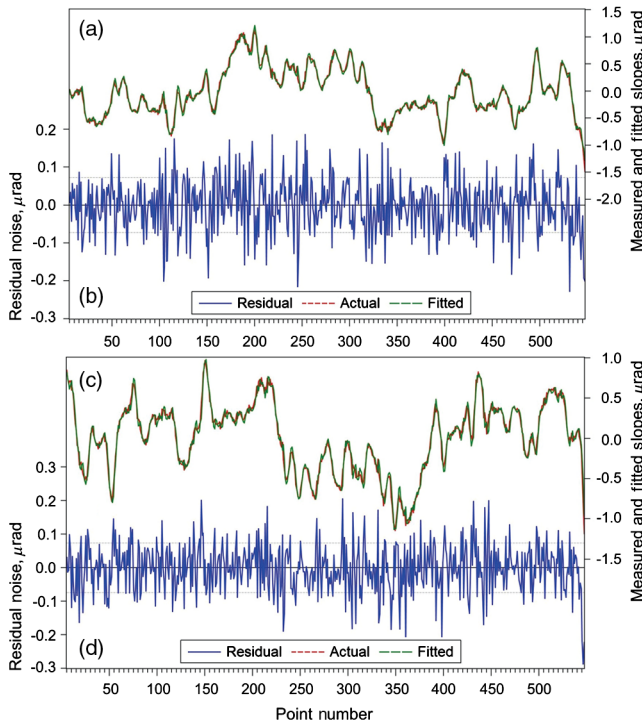


Fig. 1 (a) Measured slope trace after subtracting the best-fit spherical surface shape with a radius of curvature of 1287.5 m (the red short-dashed line); and best-fitted slope trace, corresponding to the ARMA model specified in Table 1 (the green long-dashed line). The root mean square (RMS) variation of the measured slope trace is $0.447 \mu\text{rad}$. (b) Residual noise trace equals to the difference between the measured and fitted traces in plots (a). The RMS variation of the residual noise in plot (b) is $0.073 \mu\text{rad}$. (c) Reversed measured slope trace (the red short-dashed line); and best-fitted slope trace, corresponding to the ARMA model specified in Table 2 (the green long-dashed line). (d) Residual noise trace equals to the difference between the measured and the fitted traces in plots (c). The RMS variation of the residual noise in plot (d) is $0.074 \mu\text{rad}$. Note that in the both cases the measured and the best-fit traces are almost exactly overlapped. The measurement was performed with an increment of 0.2 mm .

coefficients are highly significant at $< 1\%$ significance level. EViews also report various criteria to be helpful as a model selection guide, for example, when examining the number of regression lags.⁷

Standard ARMA modeling is inherently causal, assuming that the current value of the process only depends on the past, as expressed with Eq. (1). While in the case of the time series, the property of causality is natural, in the case of the modeling surface metrology data, the causality can be thought of as a limitation of the modeling. Below, we suggest a simple way for fixing the causality problem.

First, let us apply the same ARMA model to the reversed residual slope trace, traces (c) and (d) in Fig. 1. The reversed data correspond to the DLTP measurements with the optic rotated (flipped) by 180 deg with respect to the scanning direction of the profiler. In order to reverse the residual slope trace, we transform the coordinate system related to the mirror surface and change the measured slope values to the opposite sign (see Ref. 24). The parameters of the corresponding best-fitted ARMA model are presented in Table 2.

The residual noise traces shown in Fig. 1, plots (b) and (d), are the driving noise of the model $v[n]$ in Eq. (1) and should be distinguished from any observation noise. According to the ARMA definition, the driving noise must be uncorrelated and normally distributed. The correlation analysis performed indicates uniform ACFs for both fits. The driving noise of the ARMA modeling of the normally oriented slope trace [plots (a) and (b) in Fig. 1] passes a number of criteria, including the Jarque-Bera statistic test, for normally distributed variables.^{9,10} This is not the case for the ARMA modeling of the reversed slope trace. A rather high Jarque-Bera statistic parameter (8.69) and a low probability value (0.013) indicate that, most probably, the residuals are not normally distributed. However, for the purpose of the present work this does not produce a problem, because the variance of the noise is much smaller than the overall slope data variance described with the model.

As the second step of fixing the causality problem, let us note that the ARMA modeling of the direct and the reversed residual slope traces effectively establishes a relation between the current slope element $\alpha[n]$ and the "future" ones rather than a negative lag value:

$$\alpha[n] = \sum_{l=1}^p a_l^* \alpha[n+l] + \sum_{l=0}^q b_l^* v[n+l], \quad (8)$$

where for the direct slope trace $\alpha[n]$, a_l^* and b_l^* denote the ARMA parameters determined by the modeling of the reversed trace. Therefore, the causality limitation can be solved by a straightforward averaging of the causal stochastic processes (1) and (8) to a "two-sided symmetrical ARMA" model of the 1-D slope trace:

$$\alpha[n] = \frac{1}{2} \left\{ \sum_{l=1}^p \hat{a}_l (\alpha[n+l] + \alpha[n-l]) + \sum_{l=0}^q \hat{b}_l (v[n+l] + v[n-l]) \right\}, \quad (9)$$

where the model parameters \hat{a}_l and \hat{b}_l , given in Table 3, are the averages of the corresponding parameters in Tables 1 and 2. The values of standard errors in Table 3 are also averaged,

Table 1 Parameters of the ARMA model [(the green long-dashed line in Fig. 1(a)], which best fit the surface slope trace for the 1280 m spherical reference mirror measured with the ALS DLTP.²⁰ In Eqs. (1)–(5), $b_0 = 1$ and σ^2 is equal to the standard error (SE) of the regression of 0.073 μrad root mean square (RMS). The data in the table are regression outputs generated by EViews 8 software. Note that the values of the ARMA parameters presented here are slightly different from that of the Refs. 9 and 10, where software version 7 was used. However, the difference is well within the confidence interval for the parameters.

| Variable | Coefficient | Standard error | <i>t</i> -statistic | Probability |
|----------------------------------|-------------|--|---------------------|-------------|
| AR(1): a_1 | 1.089987 | 0.026840 | 40.61026 | 0.0000 |
| AR(4): a_4 | -0.118806 | 0.026415 | -4.497622 | 0.0000 |
| MA(2): b_2 | 0.353328 | 0.044434 | 7.951686 | 0.0000 |
| MA(3): b_3 | 0.159281 | 0.047287 | 3.368412 | 0.0008 |
| MA(6): b_6 | -0.134884 | 0.042316 | -3.187512 | 0.0015 |
| <i>R</i> -squared | 0.973392 | Mean-dependent variation | | -0.016092 |
| Adjusted <i>R</i> -squared | 0.973195 | Standard deviation-dependent variation | | 0.443422 |
| Standard error of the regression | 0.072599 | Akaike info criterion | | -2.398578 |
| Sum squared residuals | 2.835555 | Schwarz criterion | | -2.359010 |
| Log likelihood | 656.2140 | Hannan–Quinn criterion | | -2.383107 |
| Durbin–Watson statistics | 2.007877 | | | |

Note: Dependent variable: SLOPE; Method: least squares; Included observations: 543 after adjustments; Convergence achieved after 10 iterations.

rather than being decreased by a factor of $\sqrt{2}$, compared to the standard errors of the ARMA parameters determined in the corresponding regressions. This accounts for the fact that the regressions are performed over the same (just mutually reversed) data and, therefore, are not independent.

In Eq. (9), we accounted for the coincidence (within their confidential intervals) of the best fitted values of the ARMA parameters for the direct and the reversed slope traces given in Tables 1 and 2, respectively. The coincidence is natural, and it is a direct outcome of the equality of the corresponding ACFs.

Table 2 Parameters of the ARMA model [(the green long-dashed line in Fig. 1(c)], which best fits the reversed surface slope trace depicted with the red short-dashed line in Fig. 1(c). $b_0 = 1$ and σ^2 is equal to the standard error (SE) of the regression of 0.074 μrad root mean square (RMS). The data in the table are the regression outputs generated by EViews 8 software.

| Variable | Coefficient | Standard error | <i>t</i> -statistic | Probability |
|----------------------------------|-------------|--|---------------------|-------------|
| AR(1): a_1 | 1.106807 | 0.027966 | 39.57745 | 0.0000 |
| AR(4): a_4 | -0.143406 | 0.026871 | -5.336806 | 0.0000 |
| MA(2): b_2 | 0.353856 | 0.045268 | 7.816931 | 0.0000 |
| MA(3): b_3 | 0.140080 | 0.047720 | 2.935475 | 0.0035 |
| MA(6): b_6 | -0.137039 | 0.042567 | -3.219367 | 0.0014 |
| <i>R</i> -squared | 0.971694 | Mean-dependent variation | | 0.002690 |
| Adjusted <i>R</i> -squared | 0.971484 | Standard deviation-dependent variation | | 0.436396 |
| Standard error of the regression | 0.073693 | Akaike info criterion | | -2.368653 |
| Sum squared residuals | 2.921692 | Schwarz criterion | | -2.329085 |
| Log likelihood | 648.0893 | Hannan–Quinn criterion | | -2.353182 |
| Durbin–Watson statistics | 1.984440 | | | |

Note: Dependent variable: SLOPE; Method: least squares; Included observations: 543 after adjustments; Convergence achieved after 10 iterations.

Table 3 Parameters of the suggested “two-sided symmetrical ARMA” model, given by Eq. (9). The values in the table are the average of the corresponding values in Tables 1 and 2. For all the values, we keep the same number of digits as in the regression outputs generated by EViews 8 software (Tables 1 and 2).

| Model parameter | Coefficient | Standard error |
|--------------------|-------------|----------------|
| AR(1): \hat{a}_1 | 1.098397 | 0.027403 |
| AR(4): \hat{a}_4 | -0.131106 | 0.026643 |
| MA(2): \hat{b}_2 | 0.353592 | 0.044851 |
| MA(6): \hat{b}_6 | -0.135962 | 0.042442 |
| MA(3): \hat{b}_3 | 0.149681 | 0.047504 |

Unlike causal, one-sided ARMA modeling, the “two-sided symmetrical ARMA” model, depicted by Eq. (9), is free of the limitations of the fixed direction (time flow) and causation. This implies that the current value of the surface slope depends on the past and the future, in our case the neighboring points with the positive and negative lag values. Such an extension of AR modeling is closely related to the TILF approach.

4 Mathematical Foundations of Time-Invariant Linear Filters in Application to Modeling of Surface Metrology

For a 1-D case, the TILF C with weights $\{c_i, i = 0, \pm 1, \dots\}$ is a linear operator that transforms one stochastic process $\{X[t], t = 0, \pm 1, \dots\}$ into another (filtered) process $\{Y[t], t = 0, \pm 1, \dots\}$ (see Ref. 25):

$$Y[t] = \sum_{l=-\infty}^{\infty} c_l X[t-l]. \tag{10}$$

Similarly to the ARMA transformation, the TILF C is linear and time invariant. The filter C possesses the property of causality if

$$c_i = 0 \quad \text{for } i < 0. \tag{11}$$

The requirement of stability of the transformation implies that the filter is absolutely summable:

$$\sum_{l=-\infty}^{\infty} |c_l| < \infty. \tag{12}$$

Similar to the ARMA modeling, when an optimal TILF is identified, the corresponding PSD distribution can be analytically derived [see Ref. 25 and compared with Eq. (5)]:

$$P_Y(f) = \left| \sum_{l=-\infty}^{\infty} c_l e^{i2\pi lf} \right|^2 P_X(f). \tag{13}$$

Any ARMA process $\alpha[t]$ with the parameters p and q can be obtained from the white Gaussian noise $\nu[n]$ by application of the corresponding casual TILF (see Ref. 25) so that:

$$\alpha[t] = \sum_{l=0}^{\infty} c_l \nu[t-l]. \tag{14}$$

The weights c_l in Eq. (14) are determined by the relation:

$$\sum_{l=0}^{\infty} c_l z^l = b(z)/a(z), \quad |z| \leq 1, \tag{15}$$

where the AR and MA polynomials in the right-hand side of Eq. (15) are, respectively,

$$a(z) = 1 - a_1 z^1 - \dots - a_p z^p \quad \text{and} \\ b(z) = 1 + b_1 z^1 + \dots + b_q z^q. \tag{16}$$

Consequently, the “two-sided ARMA” process given by Eq. (9) can be expressed via TILF in the form of Eq. (9), which is free from the causality limitation:

$$\alpha[t] = \frac{1}{2} \left\{ \sum_{l=0}^{\infty} c_l \nu[t-l] + \sum_{l=0}^{\infty} c_{-l} \nu[t+l] \right\} \\ = \sum_{l=-\infty}^{\infty} c_l^* \nu[t-l]. \tag{17}$$

Therefore, in the case of 1-D metrology data, if ARMA modeling is successful, there is a corresponding TILF operator that describes the metrology result as a filtered white Gaussian noise. The identified TILF can be used for forecasting a new slope distribution possessing the same statistical properties as the measured one, but with different parameters, such as the distribution length and the RMS variation. A straightforward generalization of the 1-D Eqs (10)–(17) to the 2-D case opens the way for parametrization and forecasting of 2-D metrology data by applying the 2-D TILF modeling.

Note that there is a simple relation between the coefficients of the AR terms of Eq. (9) and the weights of a TILF that transforms the “two-sided AR” process into the noise process $\nu[n]$. In some sense, such a TILF is the inverse operator to the one in Eq. (14). In this case, the AR part of Eq. (9) can be written as:

$$\alpha[n] = \frac{1}{2} \sum_{l=-p}^p a_l \alpha[n-l] - \frac{1}{2} a_0 \alpha[n] + \nu[n], \tag{18}$$

with the coefficients $a_l, l = \pm 1, \dots, \pm p$ determined by the AR modeling of the direct and the reversed traces of the same slope measurement $\alpha[n]$. Assigning $a_0 = -2$, Eq. (18) is rewritten in the form of a TILF transformation:

$$\nu[n] = \sum_{l=-p}^p c_l \alpha[n-l], \tag{19}$$

with the weights

$$c_l = -a_l/2, \quad \text{for } l = \pm 1, \dots, \pm p, \quad \text{and} \\ c_0 = -1, \quad \text{for } l = 0. \tag{20}$$

Generally, the values of the TILF weights with the same positive and negative lags are not necessarily equal, that is

$$c_l \neq c_{-l}. \tag{21}$$

However, among all TILFs of the same order (including AR and ARMA models), the symmetrical filter with

$$c_l = c_{-l} \tag{22}$$

provides the smallest variance of the residual noise, which is equal to the difference between the measured trace and the best-fitted TILF model. A narration of a strong mathematical proof of this statement that we have derived is out of the scope of the present article and will be presented elsewhere. In the case of causal TILFs (like AR and ARMA models), this can be intuitively understood as a result of averaging of the residual noises of the fits with the corresponding causal filters of the direct and reversed processes. Assuming that the residual noises are not mutually correlated, one should expect a suppression of the variance of the averaged residual noise by a factor of 2 with respect to the corresponding causal filter [compared with the variance of the second sum in Eq. (9)].

5 Modeling of Surface Slope Measurements with Time-Invariant Linear Filter

Figures 2(a) and 2(b) reproduce the results of the modeling of the measured slope trace in Fig. 1(a) with a symmetrical TILF given by Eqs. (19) and (20), with the weights equal to the corresponding AR coefficients of the “two-sided symmetrical ARMA” model given in Table 3:

$$c_1 = c_{-1} = -\hat{a}_1/2 = -0.545199, \\ c_4 = c_{-4} = -\hat{a}_4/2 = 0.065553, \quad \text{and} \quad c_0 = -1. \tag{23}$$

The redundant precision of the weight values in Eq. (23) is used only for consistency with the output style of the EViews 8 software used for the ARMA fitting of the measured slope data (Sec. 3). The TILF simulations in Fig. 2

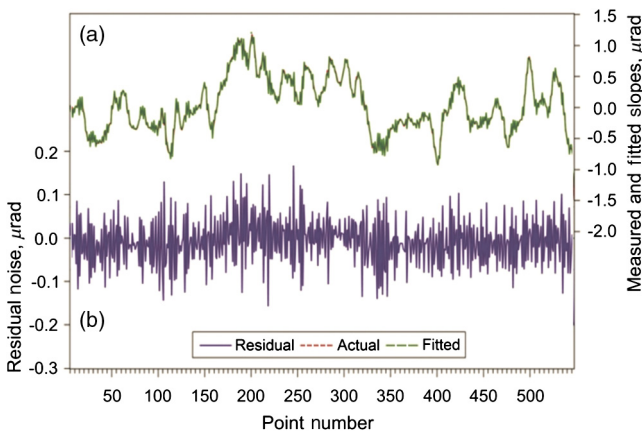


Fig. 2 (a) Measured slope trace after subtracting the best-fit spherical surface shape with a radius of curvature of 1287.5 m (the red short-dashed line); and the slope trace corresponding to the symmetrical TILF model with the weights based on the AR coefficients in Table 3 (the green long-dashed line). The RMS variation of the measured slope trace is 0.447 μrad . (b) Residual noise trace equals to the difference between the measured and the fitted traces in plots (a). The RMS variation of the residual noise in plot (b) is 0.054 μrad . Note that the measured trace and the trace simulated with the symmetrical TILF model are almost exactly overlapped. The measurement was performed with an increment of 0.2 mm.

were performed with an original code written in the MATLAB®.

A remarkable result of the modeling with the symmetrical TILF is the predicted improvement of the variance of the residual noise of the model by a factor of ~ 1.8 , compared to that of the ARMA model. Accordingly, the RMS variation of the residual noise, corresponding to the TILF model, is 0.054 μrad , rather than the 0.073 μrad in the ARMA model (Sec. 3). The improvement is slightly smaller than the factor of $\sqrt{2}$ expected for the case of the white Gaussian residual noise (see discussion in Sec. 4). This can be thought of as a signature of a small correlation within the TILF residual noise.

The high authenticity of the performed TILF modeling can be illustrated by comparing the PSD distributions of the measured and the fitted slope profiles. Figure 3 shows the analytical PSD, calculated with the symmetrical TILF model with the weights given by Eq. (23), and the PSD spectrum of the measured slope trace calculated via the discrete Fourier transform. For comparison, the analytical PSD calculated from Eq. (5) with the ARMA parameters given in Table 1 is also shown in Fig. 3.

As expected, for a single limited realization of the stochastic polishing process, the measured PSD distribution in Fig. 3 has rather poor statistical stability. This is seen as an intense frequency-to-frequency fluctuation of the spectrum. The results of the direct analytical calculations of the PSD from the coefficients of the symmetrical TILF and the best-fitted ARMA model are much smoother. They both precisely fit the noisy PSD spectrum obtained by the DFT of the measured slope data.

The analytical PSDs coincide very well over almost the entire spatial frequency range of the measurements, determined by the resolution of the slope profiler. However, there is a noticeable difference near the Nyquist frequency of about 0.7 mm^{-1} . This difference is due to the additional MA terms in the ARMA modeling. These terms effectively

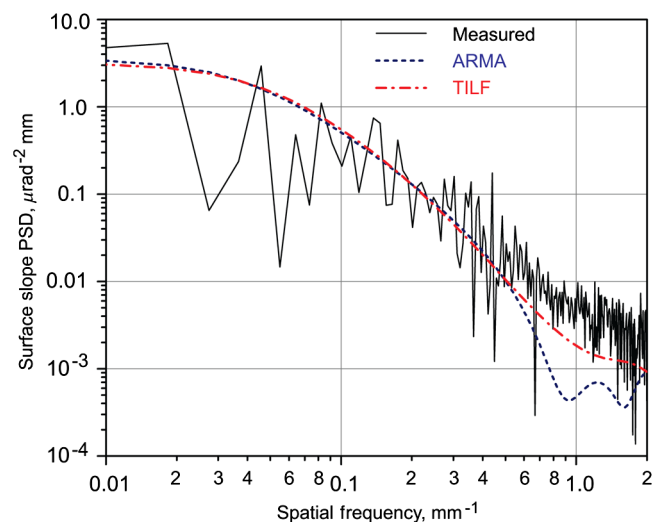


Fig. 3 TILF PSD analytically calculated with the parameters given by Eq. (23), the dash-dot red line, and the DFT PSD spectrum of the measured slope trace, the solid black curved line. For comparison, the PSD analytically calculated from Eq. (5) with the ARMA parameters given in Table 1 is also shown with the dashed blue line.

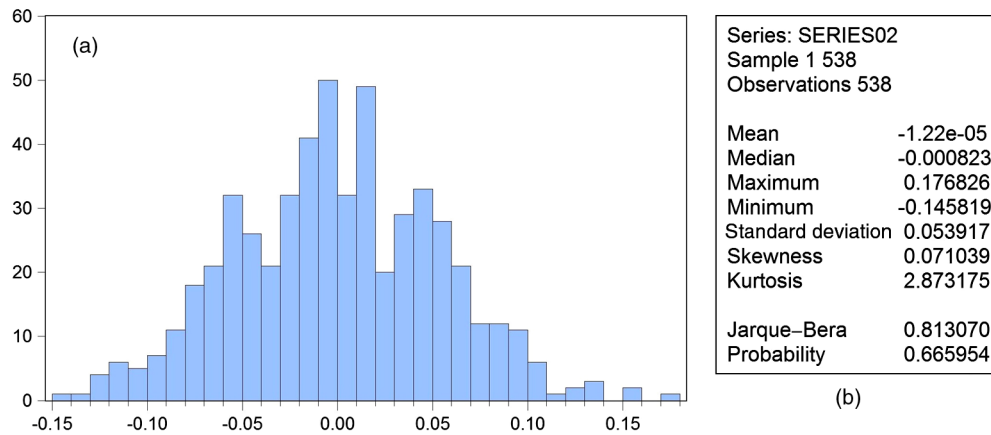


Fig. 4 Histogram normality test¹⁴ for the residual noise of the symmetrical TILF modeling shown in Fig. 2. (a) Histogram of the residuals. (b) Descriptive statistics of the residuals, including the Jarque-Bera statistic used for testing whether the residuals are normally distributed. All the descriptive statistics indicate that the residual slope is normally distributed.

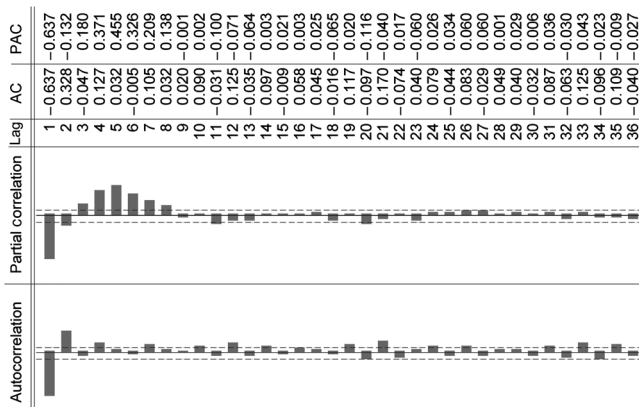


Fig. 5 EViews' output of the correlation analysis of the residual noise of modeling of the measured slope distribution, shown in Fig. 2 with the symmetrical TILF with the weights given by Eq. (23). The first 36 elements (with lag values from 1 to 36) of the autocorrelation (AC) and partial correlation (PAC) functions of the residual noise are shown. The dashed horizontal lines indicate the level of uncertainty of the correlation coefficients. A significant correlation at smaller lags is clearly seen.

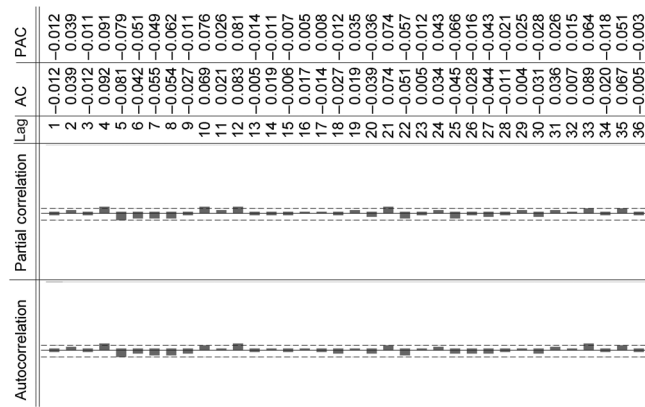


Fig. 6 EViews' output of the correlation analysis of the residual noise of the ARMA modeling of the measured slope distribution, shown in Figs. 1(a) and 1(b) with the ARMA parameters given in Table 1. The first 36 elements (with lag values from 1 to 36) of the autocorrelation (AC) and partial correlation (PAC) functions of the residual noise are shown. The dashed horizontal lines indicate the level of uncertainty of the correlation coefficients. There is no correlation on the level of significance of the modeling.

account for the noise correlation that probably appeared due to the limited resolution (oversampling) of the instrument.

The results of the statistical analysis of the TILF residual noise are presented in Figs. 4 and 5. Figure 4 reproduces the results of the EViews' normality test for the residual noise of the symmetrical TILF modeling, shown in Fig. 2. Together with other criteria, the low Jarque-Bera statistic¹⁴ and the high probability indicate that the residual noise is normally distributed.

The results of EViews' correlation analysis of the TILF residual noise are shown in Fig. 5. For comparison, similar data for the ARMA modeling in Figs. 1(a) and 1(b) are presented in Fig. 6.

From the data in Fig. 5, one can see a significant correlation in the TILF residual noise. This is a direct outcome of the applied symmetrical TILF with the weights solely based on the AR coefficients determined by the ARMA modeling. The correlation indicates that the MA-like terms of the ARMA modeling should also be incorporated in the TILF.

A direct optimization of the TILF model (without involving the results of the ARMA modeling) requires the development of dedicated software that will account for the requirement of the white Gaussian residual noise. Discussion of an algorithm of such software is out of the scope of this publication and is a topic for future investigations.

6 Conclusion

In this work, we continue the investigation started in Refs. 9 and 10, that will potentially allow the analytic characterization/parameterization of the polishing capabilities of different vendors for x-ray optics. Based on the parametrization, the expected surface profile of the prospective x-ray optics will be reliably simulated (forecast) prior to purchasing. The simulated surface slope and height distributions of the prospective beamline optics (before they are fabricated) can also be used for estimations of the expected performance of new x-ray beamlines as well as those under upgrade.

In Refs. 9 and 10, it has been demonstrated that the required reliable information about the expected surface slope topography of the prospective x-ray optics can be obtained via ARMA modeling of the 1-D slope measurements. ARMA modeling allows a high degree of confidence when fitting metrology data with a limited number of parameters. Assuming that the parameters uniquely correspond to the fabrication (polishing) technology available with a particular vendor, the determined ARMA model can be used to simulate the surface slope profile of an optic with a newly desired specification.

At the same time, with the obvious success and perspective of the application of 1-D ARMA modeling to 1-D surface slope metrology, the inherent causality of the modeling is thought of as a limitation factor that also complicates extending the method to modeling 2-D surface metrology available, for example, with high precision interferometers and microscopes.

To the best of our knowledge, we have originally suggested and performed in this work an initial consideration of the application of the TILF approach to parameterize the surface metrology of high-quality x-ray optics. We have shown that the TILF approximation has all the advantages of one-sided AR and ARMA modelings. The TILF approach, which is basically free of the causality limitation, naturally includes a "two-sided symmetrical ARMA" model that overcomes the causality problem in the frame of ARMA modeling.

Among TILFs of the same order, we have suggested applying symmetrical filters (with $c_l = c_{-l}$) that provide the smallest variance of the residual noise of the fitting. The performed numerical simulation has confirmed the high confidence of the TILF parametrization of surface slope data obtained with the high-quality reference mirror.

The major motivation of the performed investigation of the TILF-based modeling of the surface metrology data is the possibility of a direct, straightforward generalization of TILF modeling to 2-D random fields. Mathematical foundations of the generalization are well established.²⁵ However, its practical realization requires the development of calculational algorithms and dedicated software for determining the optimal TILF best-fitted to the measured 2-D surface slope and height distributions. The optimization can be done in a standard way, consisting of searching for the optimal filter's weights by using the method of least squares to minimize the variance of the residual noise. For reliable TILF forecasting of the new surface topography based on the measured and fitted ones, the residual noise of the fit has to have a zero-mean unit variance white Gaussian distribution. This is similar to the ARMA modeling, therefore, the corresponding methods and criteria can be applied to the statistical analysis of TILF modeling.

Forthcoming investigations must solve the question about the uniqueness of the ARMA and TILF parametrizations for a certain polishing process. This can be performed by cross comparing the ARMA and TILF models for different optics, which are identically fabricated. The archived metrology data for high-quality x-ray optics, collected at synchrotron facilities around the world, can be used for this purpose.

Acknowledgments

The Advanced Light Source is supported by the Director, Office of Science, Office of Basic Energy Sciences,

Material Science Division, of the U.S. Department of Energy under Contract No. DE-AC02-05CH11231 at Lawrence Berkeley National Laboratory. This document was prepared as an account of work sponsored by the United States Government. While this document is believed to contain correct information, neither the United States Government nor any agency thereof, nor The Regents of the University of California, nor any of their employees, makes any warranty, express or implied, or assumes any legal responsibility for the accuracy, completeness, or usefulness of any information, apparatus, product, or process disclosed, or represents that its use would not infringe privately owned rights. Reference, herein, to any specific commercial product, process, or service by its trade name, trademark, manufacturer, or otherwise, does not necessarily constitute or imply its endorsement, recommendation, or favoring by the United States Government or any agency thereof, or The Regents of the University of California. The views and opinions of authors expressed, herein, do not necessarily state or reflect those of the United States Government or any agency thereof, or The Regents of the University of California.

References

1. L. Assoufid et al., "Future metrology needs for synchrotron radiation grazing-incidence optics," *Nucl. Instrum. Methods A* **467–468**(1), 267–270 (2001).
2. K. Yamauchi et al., "Wave-optical analysis of sub-micron focusing of hard x-ray beams by reflective optics," *Proc. SPIE* **4782**, 271–276 (2002).
3. N. Kelez et al., "Design of an elliptically bent refocus mirror for the MERLIN beamline at the advanced light source," *Nucl. Instrum. Methods A* **582**(1), 135–137 (2007).
4. L. Samoylova et al., "Requirements on Hard X-ray grazing incidence optics for European XFEL: analysis and simulation of wavefront transformations," *Proc. SPIE* **7360**, 73600E (2009).
5. S. Moeller et al., "Photon beamlines and diagnostics at LCLS," *Nucl. Instrum. Methods A* **635**(1-1S), S6–S11 (2011).
6. E. L. Church and H. C. Berry, "Spectral analysis of the finish of polished optical surfaces," *Wear* **83**(1), 189–201 (1982).
7. S. M. Kay, *Modern Spectral Estimation: Theory and Application*, Prentice Hall, Englewood Cliffs, New Jersey (1988).
8. G. M. Jenkins and D. G. Watts, Eds., *Spectral Analysis and its Applications*, 5th ed., Emerson-Adams Press, Boca Raton, FL (2007).
9. Y. V. Yashchuk and V. V. Yashchuk, "Reliable before-fabrication forecasting of expected surface slope distributions for x-ray optics," *Opt. Eng.* **51**(4), 046501 (2012).
10. Y. V. Yashchuk and V. V. Yashchuk, "Reliable before-fabrication forecasting of expected surface slope distributions for x-ray optics," *Proc. SPIE* **8141**, 81410N (2011).
11. G. Rasigni et al., "Autoregressive process for characterizing statistically rough surfaces," *J. Opt. Soc. Am. A* **10**(6), 1257–1262 (1993).
12. B.-S. Chen, B.-K. Lee, and S.-C. Peng, "Maximum likelihood parameter estimation of F-ARIMA processes using the genetic algorithm in the frequency domain," *IEEE Trans. Signal Process.* **50**(9), 2208–2219 (2002).
13. S. Y. Chang and H.-C. Wu, "Novel fast computation algorithm of the second-order statistics for autoregressive moving-average processes," *IEEE Trans. Signal Process.* **57**(2), 526–535 (2009).
14. EViews 8 Software, "EViews 8 User's Guide, Volumes I and II, Quantitative Micro Software," <http://www.eviews.com/home.html>.
15. V. L. Popova and A. É. Filippov, "A model of mechanical polishing in the presence of a lubricant," *Tech. Phys. Lett.* **31**(9), 788–792 (2005).
16. S. M. Pandit, P. T. Suratkar, and S. M. Wu, "Mathematical model of a ground surface profile with the grinding process as a feedback system," *Wear* **39**(2), 205–12 (1976).
17. I. Fukumoto and T. Ayabe, "Improvement of ground surface roughness in Al-Si alloys," *Wear* **137**(2), 199–209 (1990).
18. A. Rommeveaux et al., "First report on a European round robin for slope measuring profilers," *Proc. SPIE* **5921**, 59210I (2005).
19. F. Siewert et al., "Global high-accuracy inter-comparison of slope measuring instruments," *AIP Conf. Proc.* **879**, 706–709 (2007).
20. V. V. Yashchuk et al., "Sub-microradian surface slope metrology with the ALS developmental long trace profiler," *Nucl. Instrum. Methods A* **616**(2–3), 212–223 (2010).
21. F. Siewert et al., "The nanometer optical component measuring machine: a new sub-nm topography measuring device for X-ray optics at BESSY," *AIP Conf. Proc.* **705**(1), 847–850 (2004).

22. F. Siewert, H. Lammert, and T. Zeschke, "The nanometer optical component measuring machine," in *Modern Developments in X-Ray and Neutron Optics*, A. Erko, M. Idir, T. Krist, and A. G. Michette Eds., pp. 193–200, Springer, New York (2008).
23. F. Siewert, J. Buchheim, and T. Zeschke, "Characterization and calibration of 2nd generation slope measuring profiler," *Nucl. Instrum. Methods A* **616**(2–3), 119–127 (2010).
24. V. V. Yashchuk et al., "Correlation analysis of surface slope metrology measurements of high quality x-ray optics," *Proc. SPIE* **8848**, 884817 (2013).
25. P. J. Brockwell and R. A. Davis, Eds., *Time Series: Theory and Methods*, 2nd ed., Springer, New York (2006).

Valeriy V. Yashchuk received his MS degree in experimental physics from St. Petersburg State University, Russia, in 1979, and his PhD degree from St. Petersburg Nuclear Physics Institute, Russia, in 1995. Currently he is leading the X-Ray Optics Laboratory at the Advanced Light Source, Lawrence Berkeley National Laboratory. He has authored more than 150 scientific publications in the fields of atomic physics, nonlinear optics, electro- and magneto-optics,

experimental scientific methods and instrumentation, and optical metrology.

Yury N. Tyurin is presently a part time professor at the Department of Probability Theory, Faculty of Mathematics and Mechanics at Moscow State Lomonosov University, Russia. He is an author of more than 100 publications and 10 books in probability and mathematical statistics. He also enjoys developing practical applications of mathematics and statistics in industry, economics, biology, etc.; some of the developments being transferred to State Standards for Industry.

Anastasia Y. Tyurina is an image processing scientist and software developer. She founded a Second Star Algonumerics company in 2008. She is presently working on commercialization of her patented method of super-resolution for detection of crowded point sources beyond the diffraction limit. She is consulting for governmental organizations and commercial companies, and in the course of the work she developed a number of patented algorithms for her clients. She graduated from Moscow State University as a mathematician.